



# Stabilization Controller Design for Differential Mobile Robot Using Lyapunov Function and Extended Kalman Filter

Tran Thuan Hoang<sup>1,2</sup>, Vo Chi Thanh<sup>1</sup>, Nguyen Ngo Anh Quan<sup>1</sup>,  
and Tran Le Thang Dong<sup>1,2</sup> (✉)

<sup>1</sup> Center of Electrical Engineering, Duy Tan University, Danang 550000, Vietnam  
nguyennanhquan@dtu.edu.vn, tranthangdong@duytan.edu.vn

<sup>2</sup> Faculty of Electrical-Electronic Engineering, Duy Tan University, Danang 550000, Vietnam

**Abstract.** This paper presents the design of a stability controller according to Lyapunov criteria in the presence of noises for a differential two-wheeled mobile robot built in the laboratory. Two Lyapunov functions are constructed that allow a hybrid feedback to control law to execute the robot movements to the desired destination from an arbitrary initial position. The asymptotical stability and robustness of the closed loop system are assured. Then, the position estimates of the Kalman filter are better than usual and designed to be inserted into the feedback control loop to improve the motion control quality. The asymptotic stability of the closed-loop control system has been proven theoretically. A variety of simulations and experiments have been carried out to prove the effectiveness and applicability of the proposed method.

**Keywords:** Kalman filter · Lyapunov function · Mobile robot control · Stabilization of mobile robot

## 1 Introduction

Researching the navigation problem for mobile robots has been interested by many authors for many years [1–11]. Success in navigation requires success at the four building blocks of navigation: perception, the robot must interpret its sensors to extract meaningful data; localization, the robot must determine its position in the environment; cognition, the robot must decide how to act to achieve its goals; and motion control, the robot must modulate its motor outputs to achieve the desired trajectory [12]. For the task of controlling the robot to track a predetermined trajectory, a simple method often used is to divide the trajectory into a set of points. Then that task will become a stable point-to-point motion control: The robot will go from the starting point to the neighboring point (sub-destination) and continue until the destination is reached. A differential mobile robot with a kinematic model as described in [13–16] is a non-holonomic system, so it will be difficult to design a static state-feedback motion control law smoothly. In addition, that control law will be invariant with time because Brockett's condition is not

satisfied [17]. Some studies have tackled this problem by using the method of converting the kinematic model to a polar coordinate system associated with navigation variables. Then, the smooth feedback control laws are introduced to control the robot to move stably from any position (coordinates and direction of the robot) to the destination position as the authors Aicardi [18], Secchi [19], ... However, those studies solely consider the ideal case when the robot model is not affected by noise, while the reality shows that the control law will no longer be stable asymptotically to the destination when there is noise, especially for input is the angular velocity. The authors [20] mentioned this problem when solving the problem of noise for a three-wheeled autonomous vehicle. Accordingly, to address the differential two-wheeled mobile robot model built with noise conditions, we also divide the robot operation configuration sets (coordinates and directions) into 2 domains: the configuration near the destination location  $(x_d, y_d, \theta_d)$  is called the local configuration set and the configuration far from the destination location is called the global configuration set [21, 22]. These results are far from perfect, especially when the robot converges to the finish line. Therefore, a new Control Law corresponding to those two configurations is proposed. Then, a Kalman filter with better position estimates is usually designed to feed into the simulated and tested feedback control loop. The result allows improving the quality of motion control.

## 2 Problem Description

Figure 1 depicts the robot's posture when it is controlled to move through 2 reference positions in the OXY global coordinate system. Attached to the robot are the  $OX_R Y_R$  local coordinate systems. The robot starts from an arbitrary position  $O_1$ , where it has coordinates  $(x, y)$  and direction angle  $\theta$ . The robot to be driven goes to the destination position  $O_2$  where it needs to have the coordinates  $(x_d, y_d)$  and the direction angle  $\theta_d$  known.

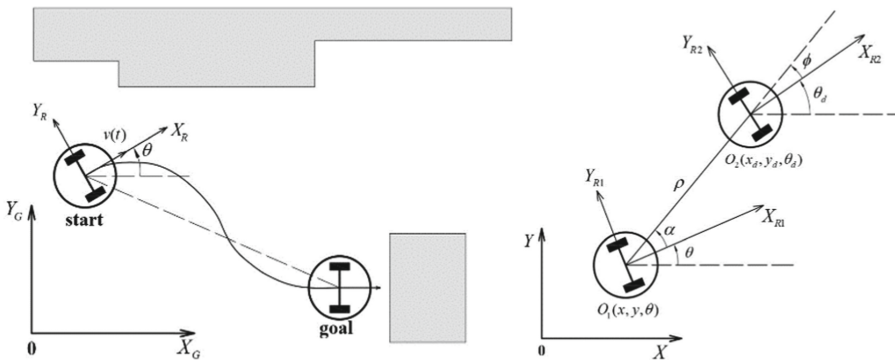


Fig. 1. Posture and parameters of the robot.

The kinematics of the robot is described as follows:

$$\dot{x} = v \cos \theta; \dot{y} = v \sin \theta; \dot{\theta} = \omega \tag{1}$$

where  $\omega$  and  $v$  are the control inputs which are respectively the rotational angular and the translational speed of the robot. Let  $O_1$  and  $O_2$  be the equilibrium points of the system of Eq. (1).

The control law according to the Lyapunov stability criterion obtained when converting the configuration variables  $(x, y, \theta)$  into navigation variables  $(\rho, \phi, \alpha)$ . With  $\rho$  be the distance between  $O_1$  and  $O_2$ ,  $\phi$  be the angular made by the vector connecting  $O_1$  and  $O_2$  and the vector connection  $O_2$  and  $X_{R2}$ ,  $\alpha = (\phi + \theta_d) - \theta$  be the angular made by the vector connection  $O_1$  and  $O_2$  and the vector connection  $O_1$  and  $X_{R1}$ .

If  $\alpha$  is in the range  $\alpha \in (-\pi/2, \pi/2)$ :

$$\begin{aligned}\rho &= \sqrt{(x_d - x)^2 + (y_d - y)^2} \\ \phi &= \text{atan2}(y_d - y, x_d - x) - \theta_d \\ \alpha &= \text{atan2}(y_d - y, x_d - x) - \theta\end{aligned}\quad (2)$$

Then the kinematic model of the robot is described through the navigation variables:

$$\begin{aligned}\dot{\rho} &= -v \cos \alpha \\ \dot{\phi} &= v \sin \alpha / \rho \\ \dot{\alpha} &= -\omega + v \sin \alpha / \rho\end{aligned}\quad (3)$$

In case  $\alpha$  is in the remaining interval  $\alpha \in (-\pi, -\pi/2] \cup (\pi/2, \pi]$ , it's possible to redefine the robot's forward direction by setting  $v = -v$ .

When there's noise, let  $\varepsilon_x, \varepsilon_y, \varepsilon_\theta$  be measured noises affecting the nominal values of coordinates  $(x, y)$  and direction angle  $\theta$ . The measured position estimates feedback to the controller will be:  $\hat{x} = x + \varepsilon_x$ ,  $\hat{y} = y + \varepsilon_y$  and  $\hat{\theta} = \theta + \varepsilon_\theta$ . Where  $|\varepsilon_x| \leq \varepsilon_x^{\max}$ ,  $|\varepsilon_y| \leq \varepsilon_y^{\max}$  and  $|\varepsilon_\theta| \leq \varepsilon_\theta^{\max}$  are bounded and  $\varepsilon_x^{\max}, \varepsilon_y^{\max}, \varepsilon_\theta^{\max}$  are the upper bounds of  $\varepsilon_x, \varepsilon_y, \varepsilon_\theta$ .

The navigation variables  $\rho, \phi, \alpha$  are also affected by the state feedback noises  $\varepsilon_\rho, \varepsilon_\phi, \varepsilon_\alpha$  as follows:

$$\begin{aligned}\varepsilon_\rho &= \sqrt{(x_d - \hat{x})^2 + (y_d - \hat{y})^2} - \sqrt{(x_d - x)^2 + (y_d - y)^2} \\ \varepsilon_\phi &= \text{atan2}(x_d - \hat{x}, y_d - \hat{y}) - \text{atan2}(x_d - x, y_d - y) \\ \varepsilon_\alpha &= \varepsilon_\phi - \varepsilon_\theta\end{aligned}\quad (4)$$

where  $|\varepsilon_\rho| \leq \varepsilon_\rho^{\max}$ ,  $|\varepsilon_\phi| \leq \varepsilon_\phi^{\max}$ ,  $|\varepsilon_\alpha| \leq \varepsilon_\alpha^{\max}$  are bounded and  $\varepsilon_\rho^{\max}, \varepsilon_\phi^{\max}, \varepsilon_\alpha^{\max}$  are the upper bounds of  $\varepsilon_\rho, \varepsilon_\phi, \varepsilon_\alpha$ .

Similarly, let  $|\varepsilon_v| \leq \varepsilon_v^{\max}$ ,  $|\varepsilon_\omega| \leq \varepsilon_\omega^{\max}$  be the input noises of the control signals  $v$  and  $\omega$ , where are the upper bounds of  $\varepsilon_v^{\max}, \varepsilon_\omega^{\max}$ ,

System of Eqs. (4) when there is input noise, it will become:

$$\begin{aligned}\dot{\rho} &= -(v + \varepsilon_v) \cos \alpha \\ \dot{\phi} &= (v + \varepsilon_v) \sin \alpha / \rho \\ \dot{\alpha} &= -(\omega + \varepsilon_\omega) + (v + \varepsilon_v) \sin \alpha / \rho\end{aligned}\quad (5)$$

### 3 Controller Design

Let  $\Omega = \{(x, y, \theta) : \rho, \alpha, \phi \in R\}$  be the set of all accessible configurations of the robot in the configuration space. Let  $\Omega_L = \{(x, y, \theta) : \rho(x, y) - \alpha(x, y, \phi) < \varepsilon_\theta\}$  be defined as the local configuration set of the robot close to the goal configuration. Let  $\Omega_G = \Omega - \Omega_L$  be the global configuration set of the robot distant from the goal configuration.

#### 3.1 Stability Control in the Global Configuration $\Omega_G$

Choose a Lyapunov function (positive definite function) built on navigation variables of the form:

$$V = V_{G1} + V_{G2} = \frac{\rho^2}{2} + \frac{\alpha^2 + h\phi^2}{2} > 0 \quad (6)$$

Notice (3), the first derivative of  $V$  is:

$$\dot{V} = \dot{V}_{G1} + \dot{V}_{G2} = \rho\dot{\rho} + (\alpha\dot{\alpha} + h\phi\dot{\phi}) = -\rho v \cos \alpha + \alpha \left[ -\omega + v \frac{\sin \alpha}{\alpha} \frac{(\alpha + h\phi)}{\rho} \right] \quad (7)$$

To satisfy the stability condition according to the Lyapunov criterion, the first derivative of  $V$  must be negative. Based on that, the control law for  $v$  and  $\omega$  is chosen as follows:

$$\begin{aligned} v &= k_v \rho \cos \alpha \\ \omega &= k_\alpha \alpha + k_v \frac{\cos \alpha \sin \alpha}{\alpha} (\alpha + h\phi) \end{aligned} \quad (8)$$

where  $k_v > 0, k > 0$  and  $k_\alpha > 0$ . This control law, provided that the effect of state feedback noise  $\varepsilon_\rho$  and  $\varepsilon_\alpha$  has the form:

$$\begin{aligned} v &= k_v (\rho + \varepsilon_\rho) \cos(\alpha + \varepsilon_\alpha) \\ \omega &= k_\alpha (\alpha + \varepsilon_\alpha) + k_v \frac{\cos(\alpha + \varepsilon_\alpha) \sin(\alpha + \varepsilon_\alpha)}{(\alpha + \varepsilon_\alpha)} [(\alpha + \varepsilon_\alpha) + h(\phi + \varepsilon_\phi)] \end{aligned} \quad (9)$$

Substitute  $\dot{\rho}$  in (7) into (8), consider  $\dot{V}_{G1}$ :

$$\begin{aligned} \dot{V}_{G1} &= \rho\dot{\rho} = -\rho(v + \varepsilon_v) \cos \alpha \\ &= -k_v \rho \cos \alpha \cos(\alpha + \varepsilon_\alpha) (\rho + \varepsilon_\rho) - \rho \varepsilon_v \cos \alpha \end{aligned} \quad (10)$$

Consider angles  $\alpha$  and  $\alpha + \varepsilon_\alpha$  in the range  $\alpha, \alpha + \varepsilon_\alpha \in (-\pi/2, \pi/2]$ , so the components  $\cos \alpha > 0, \cos(\alpha + \varepsilon_\alpha) > 0$ . In the global configuration set, there are  $\rho > 0, \rho > |\varepsilon_\alpha|$  so  $\rho + \varepsilon_\alpha > 0$ .

Continue to consider  $\dot{V}_{G2}$ :

$$\dot{V}_{G2} = \alpha\dot{\alpha} + h\phi\dot{\phi} = \alpha[-(\omega + \varepsilon_\omega) + (v + \varepsilon_v) \sin \alpha / \rho] + h\phi(v + \varepsilon_v) \sin \alpha / \rho \quad (11)$$

Let:  $A = \alpha[-(\omega + \varepsilon_\omega) + (v + \varepsilon_v) \sin \alpha / \rho]$ ;  $B = h\phi(v + \varepsilon_v) \sin \alpha / \rho$ .

Substitute the Control Law (8) when affected by state feedback noise into  $A$  and  $B$ :

$$\begin{aligned}
 A &= \alpha \left\{ [k_v(\rho + \varepsilon_\rho) \cos(\alpha + \varepsilon_\alpha) + \varepsilon_v] \frac{\sin \alpha}{\rho} - (\omega + \varepsilon_\omega) \right\} \\
 &= -k_\alpha \alpha^2 - k_\alpha \alpha \varepsilon_\alpha - \alpha \varepsilon_\omega + k_v \alpha \cos(\alpha + \varepsilon_\alpha) [\sin \alpha - \sin(\alpha + \varepsilon_\alpha)] \\
 &\quad + k_v \alpha \varepsilon_\rho \cos(\alpha + \varepsilon_\alpha) \frac{\sin \alpha}{\rho} + \alpha \varepsilon_v \frac{\sin \alpha}{\rho} - k_v h \alpha \phi \frac{\sin(\alpha + \varepsilon_\alpha)}{(\alpha + \varepsilon_\alpha)} \cos(\alpha + \varepsilon_\alpha) \\
 &\quad - k_v h \alpha \varepsilon_\phi \frac{\sin(\alpha + \varepsilon_\alpha)}{(\alpha + \varepsilon_\alpha)} \cos(\alpha + \varepsilon_\alpha)
 \end{aligned} \tag{12}$$

$$\begin{aligned}
 B &= h\phi(v + \varepsilon_v) \frac{\sin \alpha}{\rho} = h\phi \frac{\sin \alpha}{\rho} [k_v(\rho + \varepsilon_\rho) \cos(\alpha + \varepsilon_\alpha) + \varepsilon_v] \\
 &= k_v h\phi \frac{\sin \alpha}{\rho} (\rho + \varepsilon_\rho) \cos(\alpha + \varepsilon_\alpha) + h\phi \varepsilon_v \frac{\sin \alpha}{\rho} \\
 &= k_v h\phi \sin \alpha \cos(\alpha + \varepsilon_\alpha) + k_v h\phi \varepsilon_\rho \frac{\sin \alpha}{\rho} \cos(\alpha + \varepsilon_\alpha) + h\phi \varepsilon_v \frac{\sin \alpha}{\rho}
 \end{aligned} \tag{13}$$

$$\begin{aligned}
 \dot{V}_{G2} &= A + B = -k_\alpha \alpha^2 - k_\alpha \varepsilon_\alpha \alpha - \alpha \varepsilon_\omega + k_v \alpha \cos(\alpha + \varepsilon_\alpha) [\sin \alpha - \sin(\alpha + \varepsilon_\alpha)] \\
 &\quad + k_v h\phi \cos(\alpha + \varepsilon_\alpha) \left[ \sin \alpha - \frac{\alpha}{(\alpha + \varepsilon_\alpha)} \sin(\alpha + \varepsilon_\alpha) \right] + \varepsilon_v \frac{\sin \alpha}{\rho} (h\phi + \alpha) \\
 &\quad + k_v \varepsilon_\rho \left( \frac{\alpha}{\rho} + \frac{h\phi}{\rho} \right) \sin \alpha \cos(\alpha + \varepsilon_\alpha) - k_v h \alpha \varepsilon_\phi \frac{\sin(\alpha + \varepsilon_\alpha)}{(\alpha + \varepsilon_\alpha)} \cos(\alpha + \varepsilon_\alpha)
 \end{aligned} \tag{14}$$

Since  $\alpha$  is very small, the two expressions in square brackets can be approximated when  $\cos \varepsilon_\alpha \approx 1$  and  $\sin \varepsilon_\alpha \approx \varepsilon_\alpha$ .

$$\begin{aligned}
 [\sin \alpha - \sin(\alpha + \varepsilon_\alpha)] &\approx -\varepsilon_\alpha \cos \alpha \\
 [\sin \alpha - \alpha \sin(\alpha + \varepsilon_\alpha)/(\alpha + \varepsilon_\alpha)] &\approx \varepsilon_\alpha (\sin \alpha - \alpha \cos \alpha / (\alpha + \varepsilon_\alpha))
 \end{aligned}$$

Therefore (14) can be rewritten as:

$$\begin{aligned}
 \dot{V}_{G2} &= A + B \approx -k_\alpha \alpha^2 - k_\alpha \varepsilon_\alpha \alpha - \alpha \varepsilon_\omega - k_v \alpha \varepsilon_\alpha \cos(\alpha + \varepsilon_\alpha) \cos \alpha \\
 &\quad + k_v h\phi \varepsilon_\alpha \cos(\alpha + \varepsilon_\alpha) \left( \frac{\sin \alpha - \alpha \cos \alpha}{\alpha + \varepsilon_\alpha} \right) + \varepsilon_v \frac{\sin \alpha}{\rho} (h\phi + \alpha) \\
 &\quad + k_v \varepsilon_\rho \left( \frac{\alpha}{\rho} + \frac{h\phi}{\rho} \right) \sin \alpha \cos(\alpha + \varepsilon_\alpha) - k_v h \alpha \varepsilon_\phi \frac{\sin(\alpha + \varepsilon_\alpha)}{(\alpha + \varepsilon_\alpha)} \cos(\alpha + \varepsilon_\alpha)
 \end{aligned} \tag{15}$$

From (15) we can choose a coefficient  $k_\alpha$  large enough to ignore the noise  $\varepsilon_\alpha$ ,  $\varepsilon_v$ ,  $\varepsilon_\rho$  and  $\varepsilon_\phi$  (rear components) so that  $\dot{V}_{G2} < 0$  in the global configuration  $\Omega_G$ . Hence  $V_{G2}$  will converge to a non-negative finite limit and  $\alpha$  will approach a small value.

So, with the control law chosen at (8), then  $\dot{V}_G = \dot{V}_{G1} + \dot{V}_{G2} \leq 0$  is a negative semi-deterministic function and the Lyapunov function  $V_G$  is a positive function. The system will start in the global configuration and proceed in the local configuration  $\Omega_L$ .

The system Eq. (5) with the control law (7) with noise becomes:

$$\begin{aligned} \dot{\rho} &= -[k_v(\rho + \varepsilon_\rho) \cos \alpha \cos(\alpha + \varepsilon_\alpha) + \varepsilon_v \cos \alpha] \\ \dot{\phi} &= [k_v(\rho + \varepsilon_\rho) \cos(\alpha + \varepsilon_\alpha) + \varepsilon_v] \sin \alpha / \rho \\ \dot{\alpha} &= [k_v(\rho + \varepsilon_\rho) \cos(\alpha + \varepsilon_\alpha) + \varepsilon_v] \sin \alpha / \rho \\ &\quad - \left\{ k_\alpha(\alpha + \varepsilon_\alpha) + k_v \frac{\sin(\alpha + \varepsilon_\alpha)}{(\alpha + \varepsilon_\alpha)} \cos(\alpha + \varepsilon_\alpha) [(\alpha + \varepsilon_\alpha) + h(\phi + \varepsilon_\phi)] + \varepsilon_\omega \right\} \end{aligned} \quad (16)$$

### 3.2 Stable Control in Local Configuration $\Omega_L$

The control law (8) is asymptotically stable in the global configuration  $\Omega_G$ . It however is not stable in the local configuration  $\Omega_L$ . This can be proven as follows.

Assume that the navigation variable  $\rho$  goes to small parameters  $\varepsilon_P$  ( $\varepsilon_P$  same as  $\rho$ , always positive). The variables  $(\alpha, \phi)$  go to their small disturbances  $(\varepsilon_\alpha, \varepsilon_\phi)$ . The system kinematics (15) becomes:

$$\dot{\rho} = -[k_v(\varepsilon_P + \varepsilon_\rho) + \varepsilon_v] \quad (17)$$

$$\dot{\phi} = k_v \varepsilon_\alpha (1 + \varepsilon_\rho / \varepsilon_P) \quad (18)$$

$$\dot{\alpha} = k_v \varepsilon_\alpha (1 + \varepsilon_\rho / \varepsilon_P) - 2\varepsilon_\alpha (k_\alpha + k_v) - 2k_v h \varepsilon_\phi - \varepsilon_\omega \quad (19)$$

Consider the Lyapunov function and the control law remains the same as in the global configuration  $\Omega_G$ . Substitute  $\dot{\rho}$  in (17) into (10) and consider  $\dot{V}_{G1}$ :

$$\dot{V}_{G1} = \rho \dot{\rho} = k_v (-\varepsilon_P^2 - \varepsilon_P \varepsilon_\rho) - \varepsilon_P \varepsilon_v \quad (20)$$

Choose  $\varepsilon_P > |\varepsilon_\rho| + (|\varepsilon_v|/k_v)$  so that  $\dot{V}_{G1}$  is at the boundary between the global configuration and local configuration sets. When  $\rho$  approaches a small value of  $\varepsilon_P$ , the system begins to approach the boundary region and local region.

In (13), with  $k_v > 0$  as preselected and  $V_{G1} = \rho^2/2$  is bounded so  $\rho$  is also bound. Therefore, the control law of  $v$  still holds valid in the local configuration.

Let:

$$\dot{V}_{G2} = \alpha \dot{\alpha} + h \phi \dot{\phi} = \dot{V}_{G2'} + \dot{V}_{G2''} \quad (21)$$

Consider:

$$\dot{V}_{G2''} = h \phi \dot{\phi} = h k_v \varepsilon_\phi \varepsilon_\alpha (1 + \varepsilon_\rho / \varepsilon_P) \quad (22)$$

In (18) there is a finite-escape-time (there exists a finite time  $t_1$  at which  $\phi(t_1) = \infty$  when  $\varepsilon_\alpha(1 + |\varepsilon_\rho|/\varepsilon_P) > 0$ , and (19) has the same condition as (18) because  $\alpha$  is proportional to  $\phi$ ).

When  $\varepsilon_\alpha, \varepsilon_\phi > 0$  then  $\dot{V}_{G2''} > 0$ ,  $\phi$  cannot be directed to zero, which means the system will be *unstable*. Therefore, we need to redesign the controller so that the closed-loop system works stably and sustainably. With  $\alpha = (\phi + \theta_d) - \theta$ , let  $\theta_e = \theta - \theta_d$ , or from (2) has  $\theta_e = \phi - \alpha$ .

The Lyapunov function in the local configuration is otherwise selected as follows:

$$V_L = V_{L1} + V_{L2} = \frac{\rho^2}{2} + \frac{(\phi - \alpha)^2}{2} = \frac{\rho^2}{2} + \frac{\theta_e^2}{2} > 0 \quad (23)$$

The control law  $\omega$  in the local configuration of  $\Omega_L$  is re-selected as follows:

$$\begin{aligned} v &= k_v(\rho + \varepsilon_\rho) \cos(\alpha + \varepsilon_\alpha) \\ \omega &= -k_\theta \theta_e \end{aligned} \quad (24)$$

As selected in (20) (the control law  $v$  is still valid for the local configuration),  $\dot{V}_{L1} = \dot{V}_{G1} \leq 0$  and  $\alpha, \rho, \phi$  are bounded. Consider  $\dot{V}_{L2}$ :

$$\dot{V}_{L2} = \theta_e \dot{\theta}_e = \theta_e(\omega + \varepsilon_\omega) = \theta_e(-k_\theta \theta_e + \varepsilon_\omega) = -k_\theta \theta_e^2 + \theta_e \varepsilon_\omega \quad (25)$$

From (25) choose  $k_\theta$  large enough for  $\dot{V}_{L2} \leq 0$  or  $\dot{V}_L = \dot{V}_{L1} + \dot{V}_{L2} \leq 0$ . In the global configuration with control law (8), the system will start from the global configuration and move into the local configuration. When the value of  $\rho$  approaches a small value of  $\varepsilon_P$ , the system starts to switch to a local configuration with control laws (24). Since  $\dot{V}_L \leq 0$  are bounded at the boundary between the global configuration  $\Omega_G$  and local configuration  $\Omega_L$  sets, so  $\Omega_L = \{x \in R^n | V_L \leq C\}$  are bounded and the limit of  $V_L$  is  $C > 0$  when  $t \rightarrow \infty$ . Then set  $\dot{V}_{L2} \leq 0$  with  $\Omega_L = \{x \in R^n | V(x) \leq C\}$  for every  $x \in \Omega_L$  are positive invariant because every solution starting from  $\Omega_L$  will stay in  $\Omega_L$  for every  $t \geq 0$ . In other words, each trajectory starting in  $\Omega_L$  must stay in  $\Omega_L$  and converge asymptotically to the equilibrium point  $O_2$  when  $t \rightarrow \infty$ . The local configuration  $\Omega_L$  is also called region of attraction or region of asymptotic stability [23]. Then  $\rho \rightarrow 0; \theta_e \rightarrow 0; x \rightarrow x_d; y \rightarrow y_d; \theta \rightarrow \theta_d$ .

### 3.3 Using Kalman Filter for Feedback Control Loop

In [13–16], the author and research team used sensor fusion using Kalman filter to accurately position differential mobile robots. The results reveal that the estimated value of the position received from the Extended Kalman filter is closer to the nominal value of the robot than usual. This is like minimizing the effect of measurement noise.

In the motion control phase, the input noise  $(\varepsilon_v, \varepsilon_\omega)$  and the measurement noise  $(\varepsilon_x, \varepsilon_y, \varepsilon_\theta)$  significantly affect the performance of the control model such as trajectory tracking and converge to the destination domain. The author and colleagues tested the design of a closed feedback control loop in the program as shown in Fig. 2 in which a Kalman filter was introduced into the feedback line to improve the reliability of the robot position estimation. Since the state estimates at the output with the Extended Kalman filter are more reliable than those without, the deviations from the comparator output from the destination value feed to the stable controller input will have higher reliability. The result has better control quality.

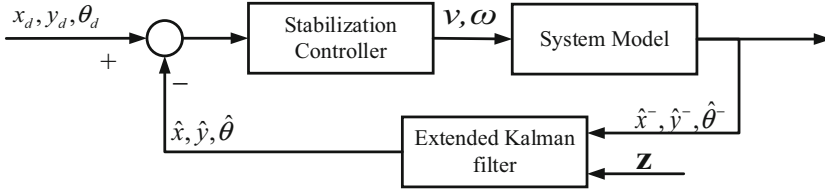


Fig. 2. Feedback control loop with Kalman filter.

Simulation and experimental results indicate that using the Extended Kalman filter in the feedback loop of the motion control system allows increasing the accuracy of the feedback value, or reducing the error and controlling the limit of the feedback noise compared to the normal case.

### 4 Simulation and Experiment

The simulation is performed in MATLAB where the parameters are extracted from the real robot built in the laboratory. The control law satisfying the Lyapunov stability criterion in both configuration sets  $\Omega_G$  and  $\Omega_L$  has been applied.

The maximum speed of the robot is 1.3 m/s, the sampling time of the system is  $\Delta t = 100$  ms. The system error when reaching the destination is  $\rho = 10^{-2}$  m.

The parameter values are selected as follows:  $k_v = 1$ ;  $k_\alpha = 2$ ;  $k_\theta = 1$  and  $h = 5$ . The measured noise values are selected based on the largest deviation in the estimate of the EKF word for the real robot which are  $\varepsilon_x^{\max} = 0.1$  m,  $\varepsilon_y^{\max} = 0.1$  m and  $\varepsilon_\theta^{\max} = 0.0036$  m. The system noise is based on the experimental investigation with real robot controlling motor by PID algorithm with the error of angular velocity  $\omega_L$  and  $\omega_R$  are  $\pm 5\%$ . So, for  $v_{\max} = 1.3$  m/s then  $\varepsilon_y^{\max} = 0.065$  and  $\varepsilon_x^{\max} = 0.2167$ . The  $\varepsilon_P$  value to switch to the local configuration is selected so that the condition  $\varepsilon_P \geq |\varepsilon_\rho| + (|\varepsilon_v|/k_v)$  is satisfied.

In simulation 1 when investigating the stability, we choose a robot whose destination configuration is  $(0, 0, 0^\circ)$ , starting configuration is  $(-2, 3.5, -60^\circ)$ . The robot is controlled to move stably from the starting position to the destination position. The results obtained when using only one control law (8) for both configurations are shown in Figs. 3(a), 4(a). Although the path coordinates are stable to the destination after 150 sampling time steps with coordinates  $(x, y) = (0.0032$  m,  $0.0013$  m), the direction angle  $\theta$  still exists non-zero and fluctuates strongly. While the results in Figs. 3(b), 4(b) show the efficiency when separating two configurations using control law (25) for the local configuration, all three variables have stabilized asymptotically to the destination and return to 0 for both  $(x, y, \theta) = (0.0086$  m,  $0.0035$  m,  $-0.0031$  rad).

In simulation 2, the starting position of the robot is  $(0, 0, 0^\circ)$  and the three non-zero destination positions are:  $(2, 2, 30^\circ)$ ,  $(2, 2, 60^\circ)$  and  $(2, 2, 90^\circ)$ . Figure 5(a) shows the simulation results where the destination configurations of the robot are converged to coordinates  $(2, 2)$  with three different orientation angles. This shows the feasibility of the controller.

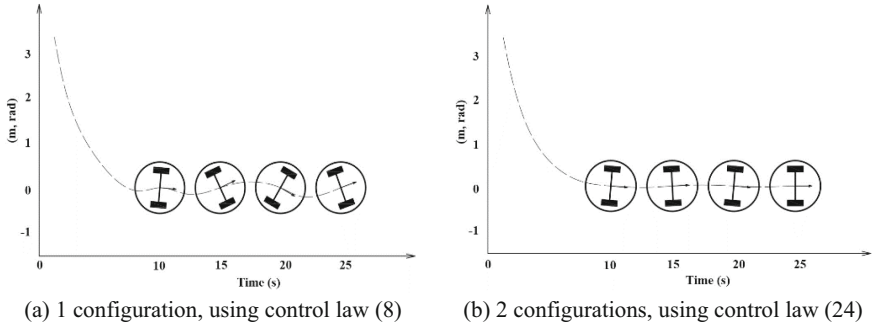


**Fig. 3.** Stabilization results with the assumption of constant measurement noises and input disturbances.

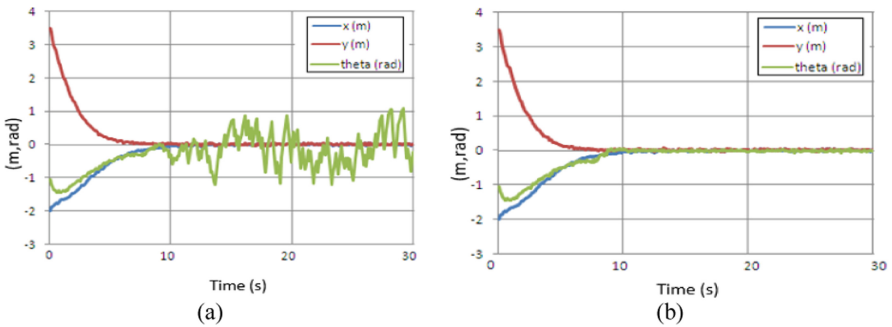


**Fig. 4.** Result response to control laws using 1 configuration (a) and 2 configurations (b).

The navigation experiment was conducted on the differential two-wheeled robot in the laboratory from the starting position to the destination position and gave satisfactory results as shown in Fig. 5(b), almost simulated.

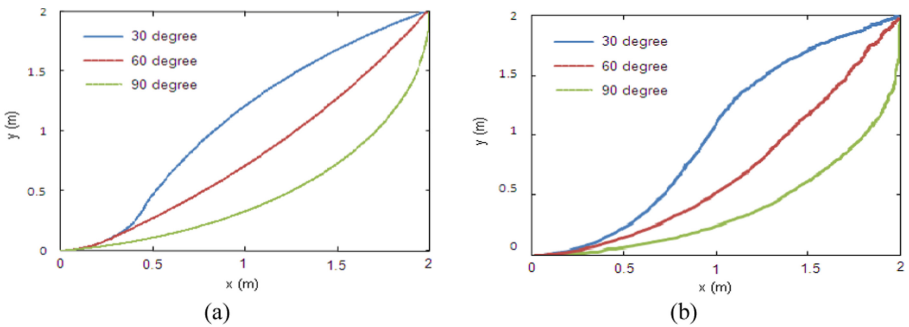


**Fig. 5.** Simulation results (a) and experimental results (b).

The stability control results of the trajectory tracking control model are convergent and the stability in the destination domain is tested in two cases:

When not using Kalman filter: measurement results in Fig. 6(a) for linear velocity  $v$  and Fig. 6(b) for angular velocity  $\omega$ .

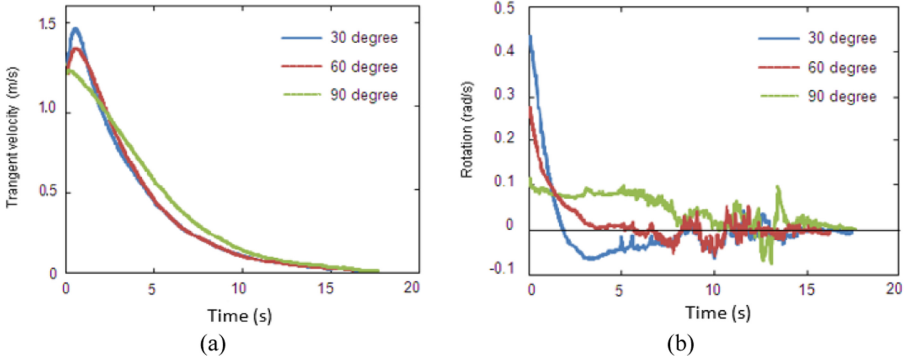


Fig. 6. Stable control results without Kalman filter.

When not using Kalman filter: measurement results in Fig. 7(a) for linear velocity  $v$  and Fig. 7(b) for angular velocity  $\omega$  (Fig. 8).

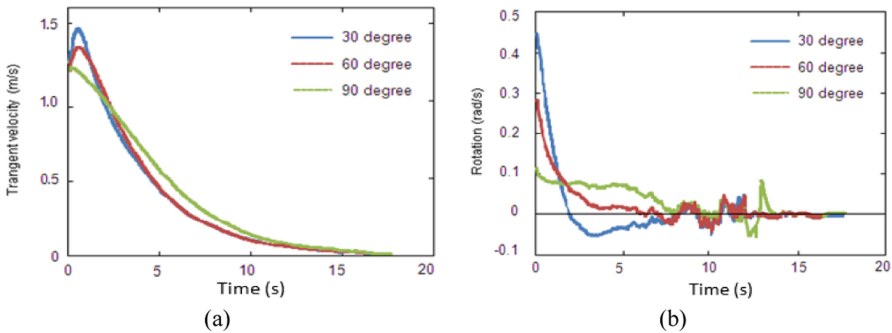
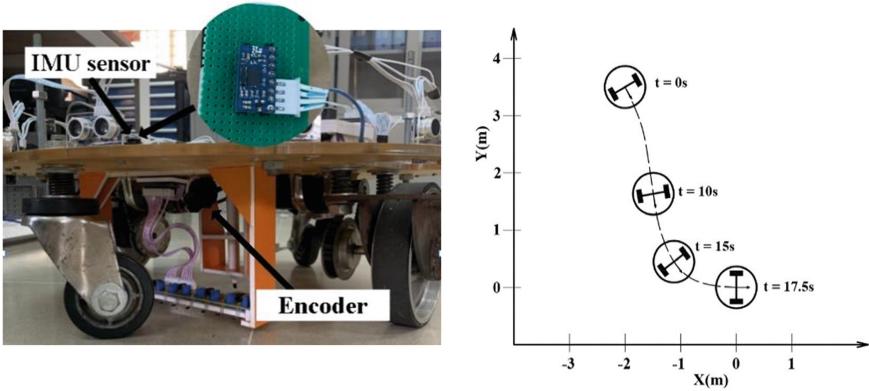
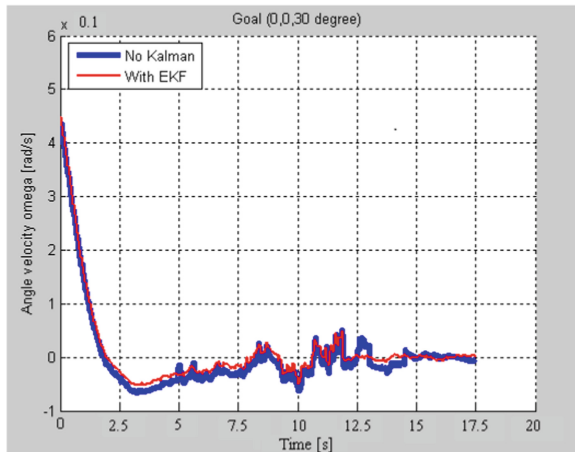


Fig. 7. Stable control results with Kalman filter.

The Fig. 9 graph extracted from the Figs. 6(b) and 7(b) graphs is a visual comparison of the variation of the velocity of angle  $\omega$  over time with and without Kalman filter when destination position is  $(0, 0, 30^\circ)$ . It can be seen that, through the Kalman filter with the sensor data fusion (red line), the estimation of the robot state (especially the direction angle) will be better, so the velocity of angle  $\omega$  of the controlled robot near the destination neighborhood is stabler than the case without Kalman filter (blue line).



**Fig. 8.** Robot used in the experiment & Experiment result: X-Y coordinates.



**Fig. 9.** The angular velocity  $\omega$  stably asymptote to the destination without the EKF (blue line) and with the EKF (red line) (Color figure online).

## 5 Conclusion

This paper presents studies on the implementation of the tracking stability control process by using the positioning values by merging the sensor's data with the EKF for motion control. As a result, the combination of using stable motion control laws in 2 sets of configurations according to Lyapunov standards with EKF allows to increase the accuracy and stability of the motion trajectory. Although the Lyapunov method may require a longer distance, in return, a continuous trajectory will be obtained, satisfying both the angle and the direction of the robot at the destination.

## References

1. Ngo, Q.H., Hong, K.-S., Jung, I.H.: Adaptive control of an axially moving system. *J. Mech. Sci. Technol.* **23**, 3071–3078 (2009)
2. Michalek, M., Kozłowski, K.: Vector-field orientation feedback control method for a differentially driven vehicle. *IEEE Trans. Contr. Syst. Technol.* **18**(1), 45–65 (2010)
3. Liang, Z., Wang, C.: Robust exponential stabilization of nonholonomic wheeled mobile robots with unknown visual parameters. *J. Control Theory.* **9**(2), 295–301 (2011)
4. Trung, T.D., Vinh, N.Q., Thuan, T.D., Hung, N.Q.: Building an algorithm to determine the navigation parameters for moving vehicles on the basis of combining angular speed gyroscope with magnetometer, speedometer and accelerometer. *J. Military Sci. Technol. Res.* **09**, 13–27 (2013)
5. Fei, L.: Two-wheel Driven AGV Path Planning and Motion Control. Hebei University of Science and Technology (2016)
6. Viet, D.T.: Autonomous vehicles applied with the algorithm of motion trajectory recognition and motion trajectory prediction. In: *Proceedings of The 5th National Conference on Mechanical Science and Technology (VCME)*, pp. 110–119, Hanoi, Vietnam (2018)
7. Son, T.A., et al.: Research and manufacture of automated guided vehicle for the service ofstorehouse. *Sci. Technol. Dev. J. Eng. Technol.* **1**(1), 5–12 (2018)
8. Kim, S., Jin, H., Seo, M., Har, D.: Optimal path planning of automated guided vehicle using Dijkstra algorithm under dynamic conditions. In: *7th International Conference on Robot Intelligence Technology and Applications (RiTA)*. IEEE (2019)
9. Hasan, H.S., Abidin, M.S.Z., Mahmud, M.S.A., Mohd, M.F.M.S.: Automated guided vehicle routing: static, dynamic and free range. *J. Int. Eng. Adv. Technol.* **8**(5C), 1–7 (2019)
10. Ryck., D.M., Mark., V., Debruwere, F.: Automated guided vehicle systems, state-of-the-art control algorithms and techniques. *J. Manuf. Syst.* **54**, 152–173 (2020)
11. Moshayedi, A.J., Roy, A.S., Liao, L.: PID tuning method on AGV (automated guided vehicle) industrial robot. *J. Simul. Anal. Novel Technol. Mech. Eng.* **12**(4), 53–66 (2020)
12. Roland, S., Nourbakhsh Illah, R.: *Introduction to Autonomous Mobile Robots*, pp. 291–298. The MIT Press Cambridge, Massachusetts London, England (2004)
13. Hoang, T.T., Hiep, D.T., Duong, P.M., Van, N.T.T., Viet, D.A., Vinh, T.Q.: Development of an EKF-based localization algorithm using compass sensor and LRF. In: *Proceeding of IEEE 12th International Conference on Control, Automation, Robotics and Vision, ICARCV*, pp. 341–346 (2013)
14. Hoang, T.T., Hiep, D.T., Duong, P.M., Van, N.T.T., Viet, D.A., Vinh, T.Q.: Multi-sensor perceptual system for mobile robot and sensor fusion - based localization. In: *IEEE 1st International Conference on Control, Automation and Information Sciences (ICCAIS-2012)*, pp. 259–264 (2012)
15. Hoang, T.T., Hiep, D.T., Duong, P.M., Van, N.T.T., Duong, B.G., Vinh, T.Q.: Proposal of algorithms for navigation and obstacles avoidance of autonomous mobile robot. In: *Proceedings of IEEE 8th Conference on Industrial Electronics and Applications (ICIEA-2013)*, pp. 1308–1313 (2013)
16. Thanh, V.C., Dong, T.L.T., Quan, N.N.A., Hoang, T.T.: Autonomous vehicle navigation using inertial sensors and virtual path. In: *National Conference “High- Tech Application in Practice in 2021”* (2021)
17. Brockett, R.W.: Asymptotic stability and feedback stabilization, In: *Differential Geometric Control Theory*, Boston, Birkhauser, pp. 181–191 (1983)
18. Aicardi, M., Casalino, G., Bicchi, A., Balestrino, A.: Closed loop steering of unicycle-like vehicles via Lyapunov techniques. *IEEE Robot. Autom. Mag.* **2**(1), 27–35 (1995)

19. Secchi, H., Carelli, R., Mut, V.: An experience on stable control of mobile robots. *J. Latin Am. Appl. Res.* **33**(4), 379–385 (2003)
20. Widyotriatmo, A., Keum-Shik, H., Prayudhi Lafin, H.: Robust stabilization of a wheeled vehicle: hybrid feedback control design and experimental validation. *J. Mech. Sci. Technol.* **24**(2), 513–520 (2010)
21. Hoang, T.T., Duong, P.M., Tinh, N.V., Vinh, T.Q.: A path following algorithm for wheeled mobile robot using extended Kalman Filter. In: *IEICE Proceedings of the 3rd International Conference on Integrated Circuit Design*, pp. 179–183 (2012)
22. Tran, T.H., Phung, M.D., Van Nguyen, T.T., Tran, Q.V.: Stabilization control of the differential mobile robot using Lyapunov function and extended Kalman Filter. *J. Sci. Technol.* **50**(4), 441–452 (2012)
23. Khalil, H.K.: Chapter 3-Lyapunov Stability. *Nonlinear System*, Prentice Hall, Inc, New Jersey, p. 114 (1996)